# Monitoring Aerosols above Clouds

**Candidate Number:** 1033822
**Project number:** B8_01
**Supervisors:** Dr. A. C. Povey, Prof. R. G. Grainger

**Abstract**

A simple radiative transfer model to calculate the top-of-atmosphere (TOA) reflectance of a plane-parallel atmosphere is presented. The model uses the Discrete Ordinate Radiative Transfer software package to solve the radiative transfer equation for atmospheric layers of Rayleigh scattering air molecules, liquid water clouds, and aerosols and approximates the Earth's surface as a Lambertian reflector. Calculating TOA reflectance for two wavelengths (0.56 µm and 1.59 µm), the model is used to simulate the retrieval of cloud properties. An interpolation method is implemented to evaluate the influence of a layer of aerosol above a cloud on the retrieval of the cloud's effective radius. In particular, the sensitivity of the cloud retrieval to a layer of 0.1 µm smoke aerosol of varying optical depths is examined.

## 1 Introduction

Clouds and aerosols contribute the largest source of uncertainty to estimates and interpretations of the Earth's radiation budget [1]. An aerosol is defined as a suspension of solid or liquid particles in a gas. Sources of atmospheric aerosols can be natural (e.g. sea spray) or anthropogenic (e.g. particulates from combustion); some aerosols (e.g. biomass aerosols) can originate from either a natural or an anthropogenic source. The effect of aerosols on the radiative balance of the atmosphere can be direct or indirect. The direct effect relates to the scattering and absorption of radiation by atmospheric aerosol particles. The indirect effect includes the impact of aerosols on cloud microphysics in phenomena such as the Twomey effect [2].

Although information of cloud and aerosol properties can be obtained from in situ measurements, remote sensing from satellites provides unmatched spatial and temporal coverage of the Earth. The process of inferring the state of the atmosphere from a set of remote measurements is known as a retrieval. Nakajima and King presented a method for determining the optical depth and effective radius of a stratiform cloud layer from reflected solar radiation [3], which has become a common approach used in modern cloud retrievals [4]. In atmospheric profile retrievals, the number of estimated parameters is often greater than the number of degrees of freedom provided by measurements. Prior knowledge, in the form of a priori constraints, must therefore be applied to stabilise the retrieval. However, these constraints must be chosen carefully as they determine which of the various degenerate atmospheric profiles is a preferred solution.

The Optimal Retrieval of Aerosol and Cloud (ORAC) retrieval scheme uses an optimal estimation scheme to determine the most accurate atmospheric profile from the top-of-atmosphere (TOA) radiances measured by satellite borne visible-IR radiometers [5]. ORAC's radiative transfer model uses the Discrete Ordinate Radiative Transfer (DISORT) software package [6] to solve the radiative transfer equation for a range of atmospheric compositions and sun-satellite viewing angles. However, the current algorithm does not attempt to retrieve an atmospheric profile containing both aerosols and clouds. Retrieving aerosols in only clear-sky conditions reduces the completeness of data sets. Previous work has been done on methods to retrieve aerosols and clouds simultaneously [7], which continues to be an active area of research. In addition, if not accounted for, the presence of aerosols can impact the retrieval of cloud properties.

This report concerns the direct influence of aerosols above clouds (AAC) on TOA reflectance and hence the retrieval of cloud properties. The report is split into two main sections. The first section outlines the creation of a radiative transfer model used to calculate TOA reflectance for a given state of the atmosphere and planet. The model is a simplified version of that used by the ORAC retrieval scheme. The second section describes the cloud retrieval algorithm, based on the method presented by Nakajima and King, that is used to evaluate the sensitivity of cloud retrievals to perturbations from AAC. The aim of this analysis is to quantify the aerosol loading required to have an adverse impact on the retrieval of

cloud properties. The assumptions and limitations of both the model and retrieval method are discussed throughout the report.

# 2 The Radiative Transfer Model

The purpose of this section is to introduce the basic concepts of radiative transfer and how they are used to construct a radiative transfer model. The radiative transfer model presented in this report is based on the 'forward model' used in the ORAC retrieval scheme [5]. Optical properties of the constituents are first considered individually before being combined to form a plane-parallel atmospheric profile. Similar to the forward model, this radiative transfer model uses DISORT to solve the radiative transfer equation. Using this model, calculations of the TOA reflectance for an atmosphere containing a liquid water cloud are carried out. For a more in-depth explanation of radiative transfer and cloud physics, readers are referred to textbooks [8] [9].

## 2.1 Modelling Scattering and Absorption

Scattering is a physical process by which a particle in the path of an electromagnetic wave continuously abstracts energy from the incident wave and reradiates that energy in all directions. The scattering phase function, $F(\theta)$, describes the angular distribution of scattered light intensity, where $\theta$ is the scattering angle. Scattering is often accompanied by absorption, where incident radiation is converted into thermal energy. The scattering and absorption make up the total attenuation of light called the particle extinction. The single-scattering albedo (SSA), $\omega$, is defined as the ratio of the scattering efficiency of a particle to its extinction efficiency.

The scattering and absorption of a particle are determined by its size and chemical composition, as well as the wavelength of incident radiation. For spherical particles, the impact of particle size on scattering is inferred from its dimensionless size parameter, $x$,

$$x = \frac{2\pi r}{\lambda}, \tag{1}$$

where $r$ is the radius of the particle and $\lambda$ is the wavelength of the incident radiation. Scattering by particles in the regime $x \ll 1$ is called Rayleigh scattering. The Rayleigh scattering phase function is given by,

$$F(\theta) = \frac{3}{4}(1 + \cos^2\theta). \tag{2}$$

For Rayleigh scattering, the SSA is one. Mie scattering is an exact formulation for the scattering of plane-polarised light by a spherical particle. Therefore, Mie scattering can be used for spherical particles of arbitrary size; Rayleigh scattering is recovered from the Mie solution as $x$ tends to zero. Due to the relative simplicity of its mathematical form, Rayleigh scattering is used when it is appropriate.

In practical terms, for visible light, scattering from air molecules can be described using Rayleigh scattering, whereas scattering from aerosols and liquid clouds are described using Mie scattering. Code to calculate the Mie scattering properties with respect to size and refractive index in the IDL programming language can be found online [1]. The scattering phase function is expressed as an expansion of Legendre polynomials, $P_l$,

$$F(\theta) = \sum_{l=0}^{\infty}(2l+1)a_l P_l(\cos\theta), \tag{3}$$

where $a_l$ are the expansion coefficients. For the Rayleigh scattering phase function, all the Legendre expansion coefficients are zero, except $a_0 = 1$ and $a_2 = {}^1/_{10}$.

This model uses the ORAC aerosol classes; the four ORAC aerosol classes considered in this report

[1] Available at: http://eodg.atm.ox.ac.uk/MIE [Accessed 18 Mar. 2021]. Details of the code are given in [10]

| Name | Descriptive Name | Mixing State (Fine:Coarse) | Coarse | Fine |
|---|---|---|---|---|
| A70 | Dust | 99.0:1.0 | 100% dust | 12.5% strongly-absorbing |
| A76 | Clean Maritime | 99.0:1.0 | 100% sea-salt | 100% weakly-absorbing |
| A77 | Dirty Maritime | 99.5:0.5 | 50% dust | 12.5% strongly-absorbing |
| A79 | Smoke | 100.0:0.0 | - | 37.5% strongly-absorbing |

Table 1: The composition of the ORAC aerosol classes considered in this report. Six additional classes are used in operational work but are omitted here for brevity. The Fine:Coarse ratio, and percentage mixtures of the coarse and fine modes are in terms of particle number [11] [12].

are described in Table 1. A log-normal distribution is used to characterise the size distribution of atmospheric aerosols [13] as shown in Appendix A. Liquid clouds are modelled as a collection of spherical water droplets. A modified gamma distribution is used to characterise the size distribution of the water droplets that form liquid clouds [14] as shown in Appendix B. The effective radius, $r_e$, of both water droplets and aerosols is defined as the ratio of the 3rd and 2nd moments of the size distribution, $n(r)$,

$$r_e = \frac{\int_0^\infty r^3 n(r)\, dr}{\int_0^\infty r^2 n(r)\, dr}. \tag{4}$$

The effective radius is an important quantity as it defines the size of the aerosols and water droplets in this model.

Another important quantity is optical depth, $\tau$, which defines the vertical coordinate of atmospheric layers in DISORT. The optical depth of an atmospheric layer is defined as,

$$\tau = \ln\left(\frac{\phi_i}{\phi_t}\right), \tag{5}$$

where $\phi_i$ is the radiative flux incident on the layer and $\phi_t$ is the radiative flux transmitted through the layer.

## 2.2 Modelling Reflectance and Transmission

This radiative transfer model considers the atmosphere (in localised portions) to be plane-parallel, such that variations in the atmospheric profile are permitted only in the vertical direction. The equation describing the transfer of monochromatic radiation at wavelength, $\lambda$, through a plane-parallel medium is given by,

$$\mu \frac{dI_\lambda(\tau, \mu, \varphi)}{d\tau} = I_\lambda(\tau, \mu, \varphi) - S_\lambda(\tau, \mu, \varphi), \tag{6}$$

where $I_\lambda$ is the intensity along the direction $\mu, \varphi$ (where $\mu$ is the cosine of the zenith angle and $\varphi$ is the azimuth angle) at vertical optical depth $\tau$ and $S_\lambda$ is the source function.

Written in Fortran, the DISORT algorithm solves Equation 6 with a specified bidirectional reflectivity at the lower boundary [6]. A Python wrapper that enables the Fortran code to be called through a Python interface was found online; I made modifications to this code to enable the scattering phase functions to be a user input. Both the original wrapper and the modified wrapper are available on Github [2] [3]. It is important to note that the plane-parallel approximation used by DISORT is not valid for large viewing angles. In addition, the model is one-dimensional and does not consider polarisation effects.

In DISORT, when a cloud/aerosol layer is present in the atmosphere, the optical depth ($\tau_c$), SSA ($w_c$) and phase function ($F_c(\theta)$) of the combined layer are calculated using the following equations:

$$\tau_c = \tau_a + \tau_R, \tag{7}$$

[2] Original Python wrapper. Available at: https://github.com/chanGimeno/pyDISORT [Accessed 18 Mar. 2021].
[3] Modified Python wrapper. Available at: https://github.com/a5v/pyDISORT [Accessed 18 Mar. 2021].

$$\omega_c = \frac{\omega_a \tau_a + \tau_R}{\tau_a + \tau_R}, \tag{8}$$

$$F_c(\theta) = \frac{\omega_a \tau_a F_a(\theta) + \tau_R F_R(\theta)}{\tau_a + \tau_R}, \tag{9}$$

where the indices $a$ and $R$ indicate quantities associated with the cloud/aerosol and Rayleigh scattering respectively. For simplicity, this model neglects the absorption by trace gases in the atmosphere. It should be noted that retrievals are usually made in an atmospheric window where gas absorption is at a minimum.

For each layer bounded by a lower and upper pressure, $p_l$ and $p_u$, $\tau_R$ is calculated as,

$$\tau_R = \frac{\tau_{RT}(p_u - p_l)}{p_s}, \tag{10}$$

where $p_s$ is the surface pressure in hPa (its value is 1013.25 hPa) and $\tau_{RT}$ is the Rayleigh scattering optical depth for a column of atmosphere extending from the surface to the TOA, it is obtained [15] as,

$$\tau_{RT}(\lambda) = \frac{1}{117.03\lambda^4 - 1.316\lambda^2}, \tag{11}$$

where the wavelength is given in microns.

Since there is a pressure-dependence on the Rayleigh scattering optical depth, a vertical pressure distribution must be described. In this model, we make a simplifying assumption that the vertical pressure distribution, $p(z)$, is given by,

$$p(z) = p_s e^{-\frac{z}{H}}, \tag{12}$$

where $z$ is the height above the surface in km and H is a constant (its value is set to 7 km). The Rayleigh scattering optical depth is much smaller than the optical depths of clouds dealt with in this report, so this is a suitable approximation.

The underlying surface is assumed to be a Lambertian reflector with a given surface albedo (the ratio of the reflected to incident light on a surface).

### 2.3 Constraining the Model

In this report, there are five model parameters that are of interest: cloud optical depth (COD), cloud effective radius (CER), aerosol class, aerosol optical depth (AOD), and the wavelength of incident light. To better understand the sensitivity of the model to these parameters, the other model parameters are given fixed values, whereas these parameters are allowed to vary within a range of physically likely values.

The following assumptions apply for the remainder of the radiative transfer calculations in this report:

1. The vertical extent of the atmosphere is 100 km.
2. Clouds have a vertical extent of 0.5 km and are placed at 1-1.5 km in the atmosphere. Clouds in this range are considered low-lying and are likely to be entirely liquid phase. Low-lying clouds are of interest as they are more likely to have aerosols above them.
3. The range of CODs considered is from $2^{-3}$ to $2^7$ and the range of cloud effective radii considered is from 4 µm to 32 µm. These values describe the majority of physical low-lying clouds [9].
4. If an aerosol layer is present, it is placed at 2-2.3 km in the atmosphere and the aerosol effective radius is 0.1 µm. In nature, the dimensions of atmospheric aerosols are on length scales of several nanometers to tens of microns and they are highly dependent on the type of aerosol. In this report, a region of particular interest is Southeast Asia in boreal spring, where biomass burning occurs in very cloudy environments [16]. Therefore, the aerosol effective radius is chosen to be appropriate for the smoke aerosol class [17].

| Channel (μm) | Central Wavelength (μm) | Bandwidth (μm) | Averaged Instrumental Noise |
|---|---|---|---|
| 0.55 | 0.555 | 0.02 | 2.40% |
| 0.66 | 0.659 | 0.02 | 3.20% |
| 0.87 | 0.865 | 0.02 | 2.00% |
| 1.6 | 1.61 | 0.30 | 3.30% |
| 3.7 | 3.70 | 0.30 | 0.05 K |
| 11 | 10.85 | 1.00 | 0.03 K |
| 12 | 12.00 | 1.00 | 0.03 K |

Table 2: The AATSR channel locations, bandwidths, and averaged instrumental noises [19]. For visible channels the noise is given as percentage of measured TOA reflectance and given in Kelvin for infrared channels.

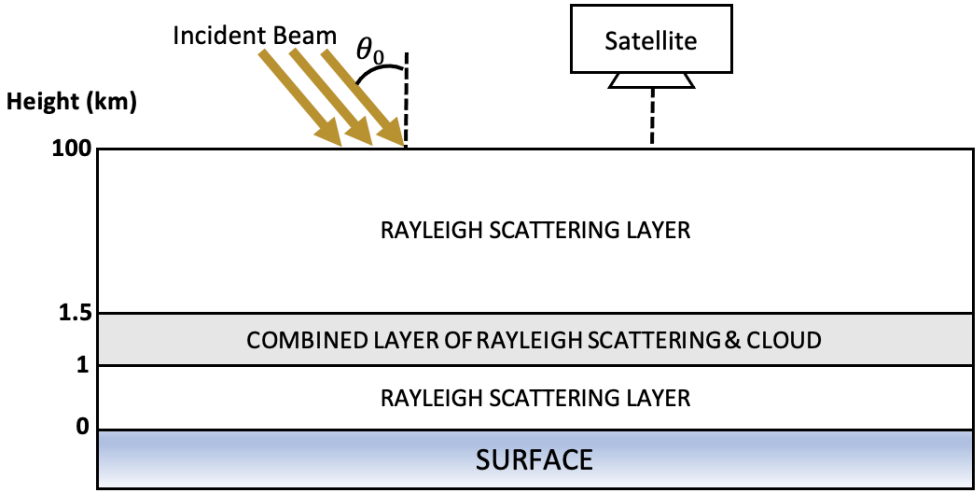


Figure 1: A schematic illustration of the vertical atmospheric profile of an unperturbed cloud used in the radiative transfer model (not to scale). $\theta_0$ is the solar zenith angle.

5. The surface albedo is set to 0.05, which is typical of an ocean surface [18].

6. The solar zenith angle and azimuthal angle are 30° and 0° respectively; the viewing zenith angle and azimuthal angle are both 0° (nadir-viewing). The nadir-viewing geometry is based on the operation of the Advanced Along Track Scanning Radiometer (AATSR) [19], which was launched on the European Space Agency's Environmental satellite platform. It should be noted that the AATSR is no longer operational.

7. The wavelengths used in the model are 0.56 μm and 1.59 μm. These wavelengths lie within two of the seven channels used by the AATSR described in Table 2.

8. The model calculates TOA reflectance. It should be noted that the physical quantity measured by the AATSR is the TOA radiance. TOA radiance can be scaled by the cosine of the solar zenith angle and normalised to produce a TOA reflectance.

## 2.4 TOA Reflectance of a Cloud

Figure 1 depicts a schematic of the atmospheric profile of an unperturbed cloud, described in Section 2.3, which is passed to the radiative transfer model. The calculated TOA reflectances for the 0.56 μm and 1.59 μm channels are shown in Figures 2a and 2b respectively. Qualitatively, increasing COD increases the TOA reflectance in both channels, but it increases to a higher value in the 0.56 μm channel. Increasing the CER has essentially no impact on the 0.56 μm channel, but decreases the reflectance in the 1.59 μm channel.

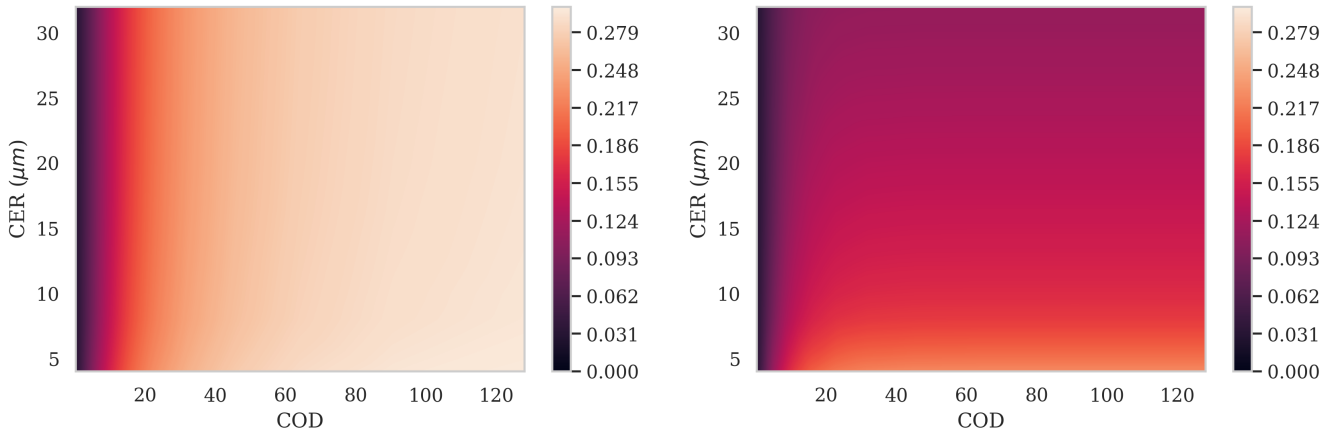


(a) TOA Reflectance in 0.56 µm channel

(b) TOA Reflectance in 1.59 µm channel

Figure 2: Theoretical calculations of TOA reflectances for an unperturbed cloud over a set of pairs of COD and CER, using the radiative transfer model.

# 3 Cloud Retrieval Simulations

In this section, a simple retrieval algorithm for CER in the absence of aerosols is presented and its sensitivity to AACs is analysed.

## 3.1 The Cloud Retrieval Algorithm

An atmospheric retrieval is an inverse problem. Given a vertical atmospheric profile, a radiative transfer model is able to calculate the TOA reflectance. A retrieval is the mathematical reversal of this process, whereby measured TOA reflectances are used to infer the most likely atmospheric profile.

Using the visible/shortwave infrared bispectral approach presented by Nakajima and King [3], this cloud retrieval algorithm determines the CER of an unperturbed cloud given the TOA reflectance of 0.56 µm and 1.59 µm solar radiation. The algorithm uses the `scipy.interpolate.griddata` module [4] to linearly interpolate $\log_{10} r_e$ of the cloud for the non-rectangular grid shown in Figure 3; the interpolation in Figure 3 is the inverse of that in Figure 2. The constraints described in Section 2.3 ensure that the values of CER, as a function of either TOA reflectance, are strictly monotonic within the range of considered values. This ensures the interpolation is well-defined within the grid of solid and dotted black lines.

## 3.2 Analysing Perturbations due to Aerosols above Clouds

The presence of atmospheric aerosols alters the scattering and absorption of solar radiation within the atmosphere. This causes the TOA reflectances, used in retrievals, to change. Therefore, unacknowledged AACs will alter the retrieved optical and microphysical properties of clouds. However, if the perturbed TOA reflectance lies within the averaged instrumental noise, the retrieval cannot distinguish the presence of the aerosol from measurement noise.

Figure 4 shows the impact of perturbations, due to different aerosol classes, on the TOA reflectance of a cloud with an effective radius of 10 µm. Qualitatively, the greater the AOD, the lower the reflectance in both channels. This illustrates that when aerosol is present, but not included in the radiative transfer model, the cloud retrieval algorithm will overestimate the CER and underestimate the COD. These biases increase with increased aerosol loading. In addition, the greater the absorption of the aerosol, the greater the perturbation to the retrieval. This is in agreement with other work on the impact of AACs [20] [21]. By inspection of Figures 4b and 4d, in this atmospheric model, the AOD required for the TOA reflectance to lie outside of the measurement error is around 0.02-0.05, depending on the absorption of the aerosol.

[4] Available at: https://docs.scipy.org/doc/scipy/reference/generated/scipy.interpolate.griddata.html [Accessed 18 Mar. 2021].

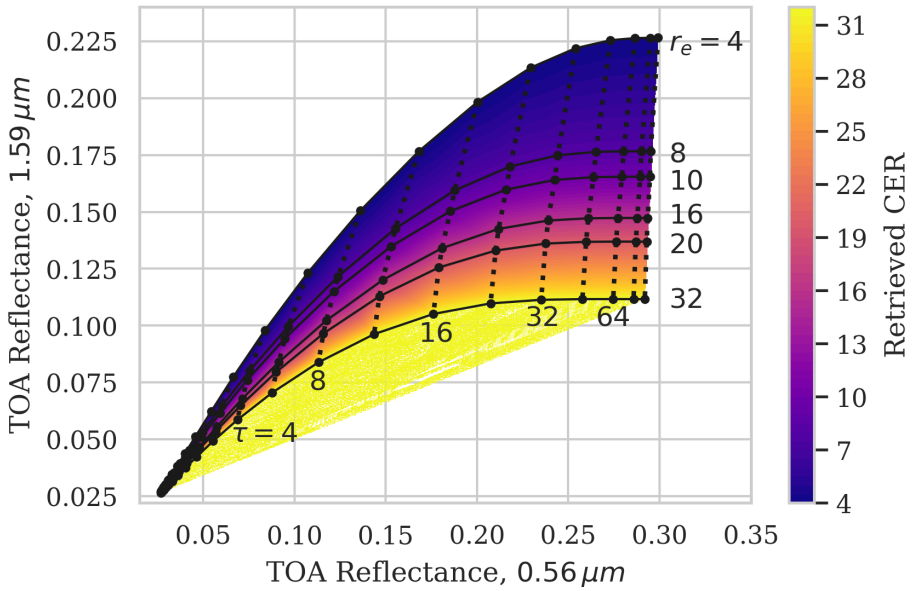


Figure 3: Contour plot showing the retrieved CER as a function of the TOA reflectances. Solid black lines are lines of constant CER and dotted black lines are lines of constant COD; selected black lines are labelled with the value held constant. The region enclosed by the grid of solid and dotted black lines forms the valid fitting region.

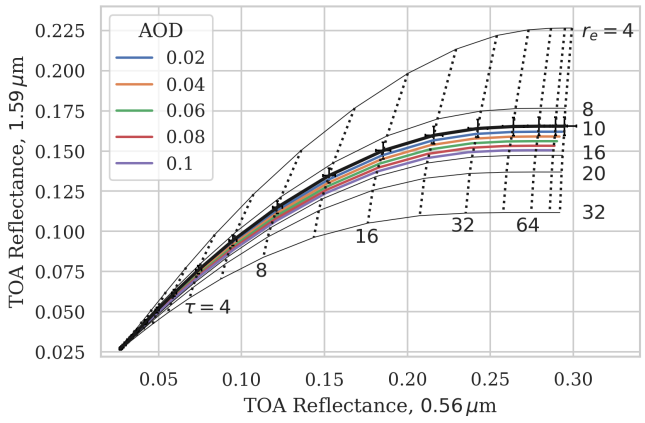


(a) Dust Aerosol (A70)

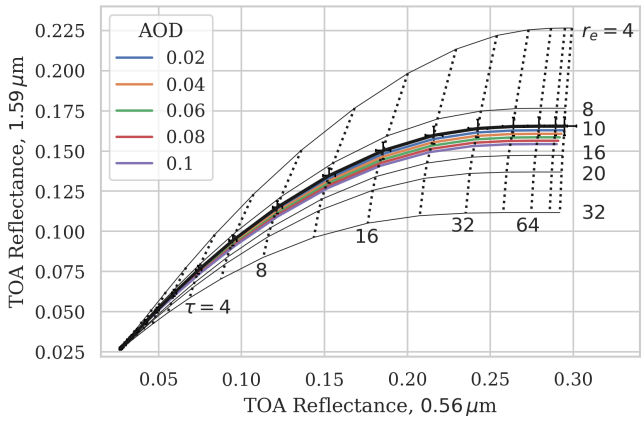


(b) Clean Marine Aerosol (A76)

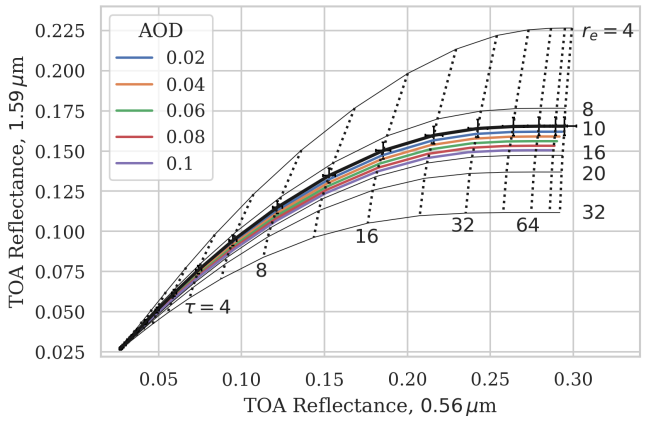


(c) Dirty Marine Aerosol (A77)

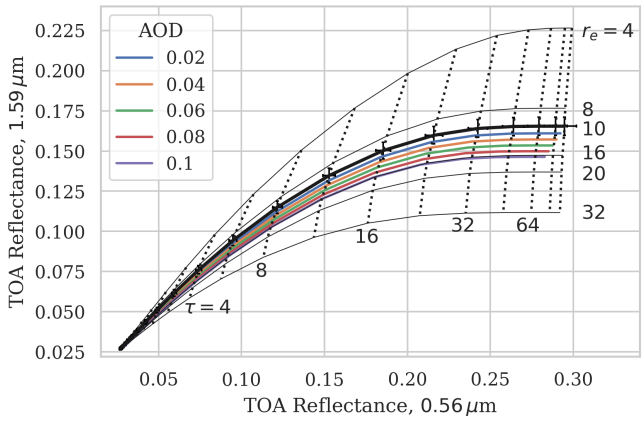


(d) Smoke Aerosol (A79)

Figure 4: The TOA reflectance of 0.56 µm and 1.59 µm solar radiation for a cloud, with an effective radius of 10 µm, that is perturbed by an aerosol. The thickest black line is the TOA reflectance for the unperturbed 10 µm cloud and the coloured lines are the TOA reflectance for the 10 µm cloud with a layer of aerosol above it for a range of AODs. The error bars represent the averaged instrumental noise for TOA values of the unperturbed 10 µm cloud. Thinner black lines are the TOA reflectances for other unperturbed clouds, which the perturbed TOA reflectances can be compared to. Each subfigure is labelled with the aerosol class used to perturb the cloud.

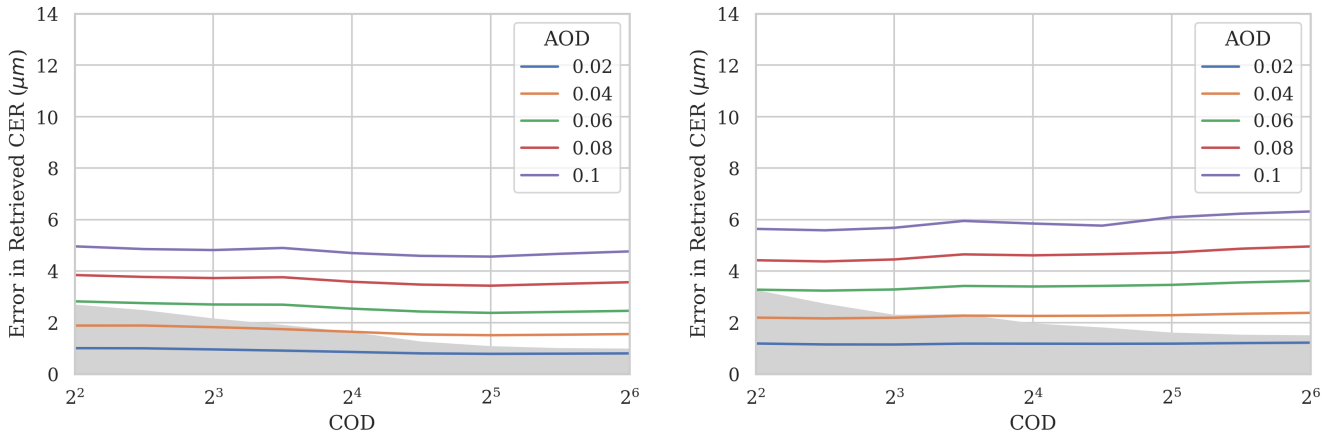


(a) 8 µm CER

(b) 10 µm CER

(c) 16 µm CER

(d) 20 µm CER

Figure 5: The error in the retrieved CER due to perturbations of 0.1µm smoke aerosol above the cloud. The coloured lines are the error in the retrieved CER over a range of AODs and the grey region represents the values of CER that could be retrieved due to instrumental noise. Each subfigure is labelled with the CER of the unperturbed cloud.

The retrieval of CER has implications for weather predictions; rain is initiated when CER near the cloud top of marine stratocumulus clouds is around 12-14 µm [22]. Figure 5 uses the cloud retrieval algorithm, described in Section 3.1, to show the error in the retrieved CER due to smoke aerosol above clouds of varying effective radii. Only optically thick clouds, with CODs greater than 4, are considered to ensure that the TOA reflectances remain within the valid fitting region of the retrieval algorithm. From these plots, the greater the COD, the lower the error in the retrieved CER due to the perturbation. However, the error effectively saturates to a constant value once a certain COD is reached. For clouds with a greater unperturbed CER, this saturation occurs at a higher COD. In the saturated region, the error on the retrieved CER increases effectively linearly with AOD. This relation is mostly independent from the initial CER of the cloud. The error in the retrieved CER due to measurement noise, for very optically thick clouds, is approximately 2 µm.

The aerosol loading required for the TOA reflectance to lie outside the instrumental error indicates the feasibility of simultaneously retrieving aerosols and clouds. Both Figures 4 and 5 show the TOA reflectance is sensitive to thin layers of absorbing atmospheric aerosol, which is in agreement with other studies [23]. This suggests a simultaneous retrieval of aerosols and clouds should be explored.

# 4 Conclusion

A radiative transfer model was created to examine the impact of a single layer of aerosol above a cloud on the retrieval of the cloud's properties. The model, which calculates the top-of-atmosphere reflectance

for a given atmospheric profile, was used to create a two-channel retrieval algorithm for cloud effective radius. For this model and retrieval algorithm, an aerosol optical depth of around 0.02-0.05, depending on the absorption of the aerosol, is required for the top-of-atmosphere reflectance to lie outside of the instrumental noise of the Advanced Along Track Scanning Radiometer; for a given aerosol optical depth, the greater the absorption of an aerosol, the greater the perturbation to the retrieval. This suggests that the retrieval is sensitive to optically thin layers of aerosols above clouds. Therefore, attempts to simultaneously retrieve aerosols and clouds, in retrieval schemes such as the Optimal Retrieval of Aerosol and Cloud, should be explored.

Although the analysis carried out in this report was fairly simplistic, the results illustrate the need to acknowledge the presence of aerosols above clouds in retrievals. To make future analysis more realistic, improvements to both the model and the retrieval method can be made. The cloud retrieval algorithm could consider a retrieval with more than two channels; operational retrieval algorithms would use at least five channels. In the model, a more accurate aerosol vertical profile could be considered. In addition, the sensitivity of the model to other parameters, such as surface albedo, should also be carried out.

## References


[1] Boucher, O. et al. (2013). Clouds and Aerosols. In: *Climate Change 2013: The Physical Science Basis.* Cambridge University Press, Cambridge.

[2] Twomey, S. (1977). The Influence of Pollution on the Shortwave Albedo of Clouds. *J. Atmos. Sci.*, 34(7):1149-1152.

[3] Nakajima, T., and King. M. (1990). Determinations of the Optical Thickness and Effective Particle Radius of Clouds from Reflected Solar Radiation Measurement. Part I: Theory. *J. Atmos. Sci.*, 47(15):1878–1893.

[4] Iwabuchi, H. et al. (2016). Retrieval of radiative and microphysical properties of clouds from multispectral infrared measurements. *Prog. in Earth and Planet. Sci.*, 3:32.

[5] Thomas, E. et al. (2009). Oxford-RAL Aerosol and Cloud (ORAC): Aerosol retrievals from satellite radiometers. In: *Satellite Aerosol Remote Sensing Over Land.* Springer, Berlin.

[6] Stamnes, K. et al. (1988). An improved and generalized discrete ordinate method for polarized (vector) radiative transfer. *Appl. Opt.*, 27(12):2502-2509.

[7] Yu, H., and Z. Zhang (2013). New Directions: Emerging satellite observations of above-cloud aerosols and direct radiative forcing. In: *Atmos. Res.* 72:36-40.

[8] Liou, K. (2002). *An Introduction to Atmospheric Radiation.* 2nd ed. Academic Press, London.

[9] Lohmann, U., Lüönd, F., and Mahrt, F. (2016). *An Introduction to Clouds.* Cambridge University Press, Cambridge.

[10] Grainger, R. et al. (2004). Calculation of Mie derivatives. *Appl. Opt.*, 43(28):5386:5393.

[11] de Leeuw, G. et al. (2017). *Algorithm Theoretical Basis Document (AATSR Oxford-RAL Aerosol and Cloud).* Available at: https://climate.esa.int/en/projects/aerosol/key-documents/ [Accessed 18 Mar. 2021].

[12] Thomas, G. et al. (2011). *Technical Note: Aerosol models.* Available at: https://climate.esa.int/en/projects/aerosol/key-documents/ [Accessed 18 Mar. 2021].

[13] Davies, C. (1974). Size Distribution of Atmospheric Particles. *J. Aerosol Sci.*, 5(3):293-300.

[14] Deirmendijian, D. (1969). *Electromagnetic Scattering on Spherical Polydispersions.* Elsevier, New York.

[15] Justus, C. and Paris, M. (1985). Modelling solar spectral irradiance and radiance at the bottom and top of a cloudless atmosphere. In: *J. Appl. Meterol.*, 24(3):193-205.

[16] Tsay, S.-C et al. (2014). From BASE-ASIA toward 7-SEA: A satellite perspective of boreal spring biomass-burning aerosols and clouds in Southeast Asia. *J. Atmos. Sci.*, 78:269-290.

[17] Li, C. et al. (2015). Evolution of biomass burning smoke particles in the dark. *Atmospheric Environment*, 120:244-252.

[18] Jin, Z. et al. (2004). A parameterization of ocean surface albedo. *Geophys. Res. Lett.*, 31(22).

[19] Huang, H. (2013). *Aerosol and Surface Properties Remote Sensing using AATSR*. Available at: http://eodg.atm.ox.ac.uk/eodg/theses/ [Accessed 18 Mar. 2021].

[20] Haywood. J. et al. (2004). The effect of overlying absorbing aerosol layers on remote sensing retrievals of cloud effective radius and cloud optical depth. *Q. J. R. Meteorol. Soc.*, 130:779-800.

[21] Coddington. O. et al. (2010). Examining the impact of overlying aerosols on the retrieval of cloud optical properties from passive remote sensing. *J. Geophys. Res.*, 115(10).

[22] Rosenfeld, D., et al. (2012). The roles of cloud drop effective radius and LWP in determining rain properties in marine stratocumulus. *Geophys. Res. Lett.*, 39(13).

[23] Sayer, A. et al. (2016). Extending "Deep Blue" aerosol retrieval coverage to cases of absorbing aerosols above clouds: Sensitivity analysis and first case studies. In: *J. Geophys. Res. Atmos.* 121(9):4830-4854.

## Appendix A Log-Normal Distribution

The log-normal distribution in terms of number density as a function of radius, $n(r)$,

$$n(r) = \frac{N_0}{\sqrt{2\pi}} \frac{1}{\sigma r} \exp\left( -\frac{(\ln r - \ln r_m))^2}{2\sigma^2} \right),$$

where $r_m$ is the median radius, $\sigma$ is the standard deviation of $\ln r$, $N_0$ is the total number density.

## Appendix B Modified Gamma Distribution

The modified gamma distribution in terms of number density as a function of radius, $n(r)$,

$$n(r) = a r^{\alpha} \exp\left(-b r^{\gamma}\right).$$

The four constants $a$, $\alpha$, $b$, $\gamma$ are real and $\alpha$ is an integer. The mode of the distribution occurs where $r = \left(\frac{\alpha}{b\gamma}\right)^{\frac{1}{\gamma}}$.